Microwave Induced Green synthesis of nanostructured ZnO as Promising Antibacterial Agent

Chauhan DS[1], Gopal CSA[1], Kumar D[2], Mahato N[3], Quraishi MA[1*] and Cho MH[3]

[1]Department of Chemistry, Indian Institute of Technology (Banaras Hindu University), Varanasi, India

[2]Department of Microbiology, Institute of Medical Sciences, Banaras Hindu University, Varanasi-221005, India

[3]School of Chemical Engineering, Yeungnam University, Republic of Korea

***Corresponding author:** MA Quraishi, Department of Chemistry, Indian Institute of Technology (Banaras Hindu University), Varanasi-221005, India, Fax: +91-542-2368428; Tel: +91-9307025126; Email: maquraishi.apc@itbhu.ac.in

Abstract

The present work reports microwave induced green synthesis of ZnO nanoparticles via hydrothermal method without using any surfactant. The protocol provides a facile and rapid method for obtaining ZnO nanoparticles having uniform particle size and high crystallinity. The synthesized nanostructures were characterized using FTIR, XRD, SEM and TEM. The synthesized ZnO nanoparticles were used to study its antibacterial behavior against common pathogenic Gram-negative bacterium *E. coli*. The results show a significant decrease in viability of pathogenic bacterial cells with increase in interaction time with ZnO nanoparticles.

Keywords: Green synthesis; Zno nanostructures; Microwave synthesis; Antibacterial activity

Introduction

Antibacterial materials typically constitute chemical compounds that locally kill bacteria or effectively slow down their growth, with no toxic effects on the surrounding tissues. While organic antimicrobial agents act relatively quicker than inorganic antibacterials, their extensive usage develops drug resistance in more and more bacteria [1-3]. In order to address this issue, inorganic metal oxides such as TiO_2, MgO, CuO, Al_2O_3, Ag_2O, CaO, CeO_2 and Zno have come forward which can act as durable antibacterial agents and provide appropriate disinfection without forming harmful by-products thereby offering key advantages of improved safety and stability as compared to organic antibiotics [2-5]. Zinc oxide is a non-toxic, n-type II-VI semiconductor material having a wurtzite structure with a direct and wide band gap of 3.37 eV. It exhibits near-UV emission, optical transparency, electrical conductivity and piezoelectricity [6,7]. Zno exhibits antimicrobial activity against a number of bacterial strains and also against various stages of bacteria such as vegetative stage and/ or spores which have a natural tendency to resist both temperature and high pressure conditions.

Microwave-assisted synthesis of inorganic nanomaterials offers benefits such as increased nucleation rates, homogeneity while heating and particularly for a controlled large-scale synthesis [8]. The microwave radiation passes through the walls of the vessel and directly heats the reactants and solvent via dipolar polarization or ionic conduction rather than heating the vessel directly [9-11]. Suitably designed vessels produce uniform heating of the sample leading to faster synthesis with higher yields and less by-products. Typical ZnO structures resulting from microwave synthesis are flower, rod, star, spindle etc. with micron scale geometry. However, there is a scarcity of available literature pertaining to the synthesis of regular Zno Np using microwave irradiation and their application in antibacterial activity.

We here in report microwave induced green synthesis of Zno Np with a homogeneous morphology and a narrow particle size distribution. The synthesis of Zno nanostructures is carried out in a domestic microwave oven by controlling the pH of medium in the absence of any surfactant and without using calcination or annealing. The structure, preferred crystallite orientation and particle size of the synthesized Np is evaluated by FTIR, XRD, SEM and TEM. Further, the antibacterial property of the Zno Np is demonstrated against a number of Gram-positive and Gram-negative pathogenic bacteria.

Experimental

Materials and instrumentation

Zn(CH$_3$COO)$_2$.2H$_2$O and NaOH were procured from Fisher Scientific. Aqueous solutions were prepared using deionized water. The strain of *E.coli* ATCC 25922 was grown at 37 °C in nutrient broth. Following this, the bacterial culture was centrifuged at 5000rpm for 15minutes. The pellets were washed with sterile physiological saline and then re-suspended in the same. From this suspension, the bacteria were inoculated in 1mL nutrient broth and the bacterial count was adjusted to approximately 0.5 McFarland. The working inoculums were further diluted 100times to obtain a concentration of 1.0×10^6 colony-forming units (CFU) mL-1.

The FTIR spectra were recorded using a Shimadzu FTIR 8400S Spectrophotometer in the range 4000 and 400cm^{-1}. X-Ray diffraction pattern of the samples were obtained by Rigaku Mini Flex 600 X-Ray diffractometer. The morphology of the samples was examined by a Zeiss EVO 18 Scanning Electron Microscope. A FEI Tecnai 20 G^2 transmission electron microscope was used to observe the high resolution microstructure.

Synthesis of zinc oxide nanoparticles

Zno Np were prepared using a microwave assisted hydrothermal method. In a typical synthesis, 2.195g Zn(CH$_3$COO)$_2$.2H$_2$O was dissolved in 100mL deionized water via ultrasonication for 5min. To this, a solution of 1 M NaOH was added drop wise with constant stirring until the pH reached 10. The mixture was then stirred for 5min to yield a milky white solution. The sample was then irradiated using a domestic microwave oven (700 W Kenstar OM-18 MSE, 2450 MHz) for 6min. The resulting white precipitates were cooled to room temperature. The samples were then filtered and washed with deionized water and ethanol followed by drying in an air oven at 60 °C for 4h. The resulting powders were collected for further analyses.

Antibacterial activity study

The microorganisms were cultivated in sterilized nutrient broth and then incubated overnight at 37 °C with a shaking incubator. For investigation of bacteriostatic performance of the prepared Zno nanoparticles, the samples were dispersed in physiological saline (1mgmL^{-1}) and subjected to ultrasonication for 15min. Then, 1mL of each suspension was placed in sterilized test tubes and inoculated with 100μL of *E. coli* suspension. The bacteria inoculated solutions were kept in an incubator in the absence of light. From each tube, 50μL aliquots were taken as a function of contact time (from 0min to 60min) and cultured in nutrient agar plates. Then, the nutrient agar plates were incubated at 37 °C for 24h, and the number of grown bacterial colonies was observed and counted.

Results and Discussion

Structural characterization

The FTIR spectra of the samples are illustrated in Figure 1a. The spectrum shows the presence of the characteristic Zn-O stretching at ~460cm^{-1} confirming the formation of ZnO [12]. A broad peak at ~3400cm^{-1} corresponds to the O-H stretching of adsorbed water molecules. The symmetric and asymmetric stretching bands from –COO$^-$ groups of acetate can be seen at 1390cm^{-1} and 1550cm^{-1} respectively. The result indicates the successful formation of zincite phase.
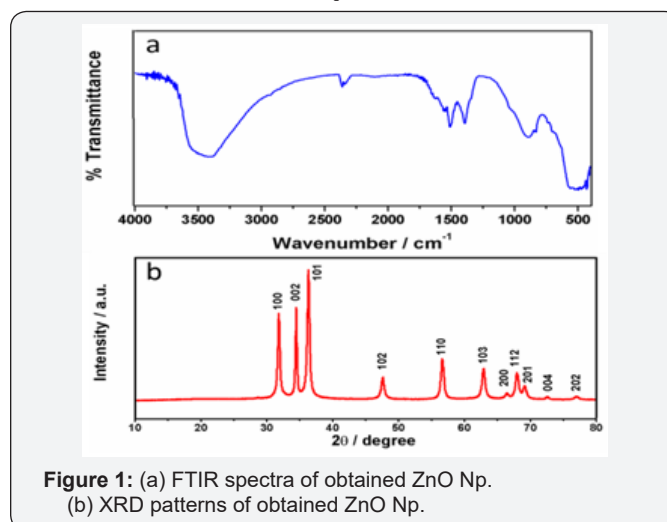

Figure 1: (a) FTIR spectra of obtained ZnO Np.
(b) XRD patterns of obtained ZnO Np.

The X-ray diffraction (XRD) pattern of the Zno Np synthesized by microwave induced hydrothermal method is shown in Figure 1b. The peaks indicate a high crystalline nature of the product which can be designated as the (100), (002), (101), (102), (110), (103), (200), (112), (004) and (202) reflections of the wurtzite-type Zno structure (JCPDS card No. 36-1451), space group (186). The results show no additional diffraction peaks either from other phases or impurities indicating purity of the synthesized material.

The crystallite size or coherence length of the material can be estimated by the Scherrer's formula [13] as shown in equation (1),
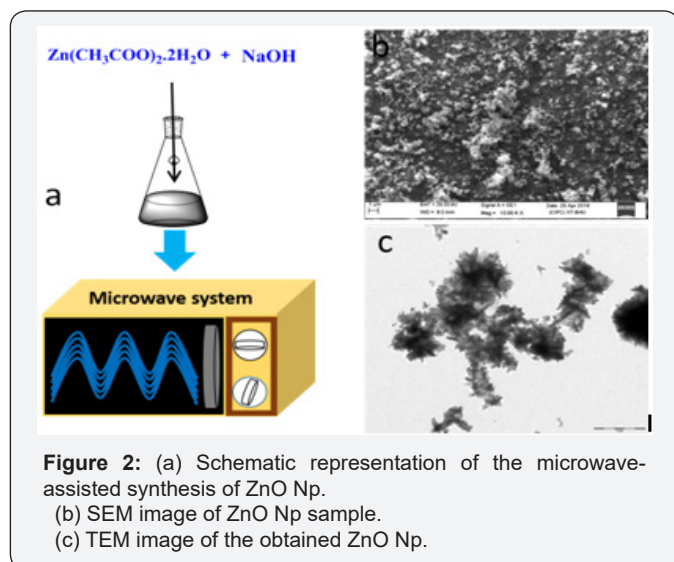
$$L_{hkl} = K\lambda / \beta_{1/2} \cos\theta \qquad (1)$$

Where K is a form factor approximately equal to unity, λ is the radiation wavelength (0.154nm for CuKα radiation), and $\beta_{1/2}$ is the full width at half maximum (FWHM) of the peak on the 2θ scale in radians. The crystallite sizes of reflections (100) and (002) are 26.4 and 39.6nm respectively. The ratio of crystallite

sizes was 1.5 indicating a small elongation of the crystallites in the direction of the c-axis, and can be attributed to the hexagonal structure of the wurtzite [14].

Morphology

Figure 2a shows a schematic of the formation process of Zno nanoparticles. The surface morphology of the synthesized nanostructures was recorded by scanning electron microscopy (SEM) as shown in Figure 2b. The samples show the formation of uniform microstructures of Zno. Slight agglomeration of the particles can be observed and the particle size can be observed to be ~100nm. In general, to obtain the different shapes of Zno via microwave processing, it is a common practice to use surfactants [15-17] and/ or aliphatic primary amines [18,19] which control the crystal growth. However, in the present condition, the synthesis was performed inside an open-mouthed flask using microwave irradiation leading to the formation of uniform small-size nanoparticles.

Figure 2: (a) Schematic representation of the microwave-assisted synthesis of ZnO Np.
(b) SEM image of ZnO Np sample.
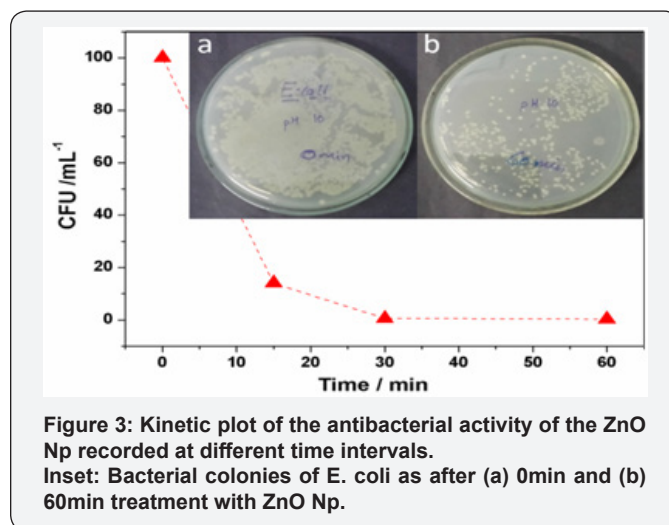(c) TEM image of the obtained ZnO Np.

The TEM image of the Zno nanoparticles is shown in Figure 2c. As can be observed, the particle size is of the order ~100nm and the Zno Np show some agglomeration. In aqueous medium Zno Np tend to aggregate and form soft agglomerates resulting from inter-particle interactions such as van der Waals, electrostatic or magnetic forces [20]. However, the particle agglomeration does not create problem for the application because the antibacterial activity of the Zno Np depends upon the size of the particles and not on the agglomerate size. Moreover, the ultrasound process can break the agglomerates of the Np in suspension.

Antibacterial activity

A number of articles are available describing the antibacterial activity of Zno Np [20-23]. However, in most of the reports the synthesis of Zno Np is carried out using high temperature wet chemical methods in the presence of various stabilizers for morphology control [20-25]. In the present work, the Zno Np were synthesized in the absence of any capping agents or polymeric stabilizers which can either passivate the surface defects of Zno or act as free radical scavengers and hence exert negative influence on the antibacterial activity of Zno. Moreover, the bacterial growth medium can cause hindrance in adherence of Zno Np to the bacterial cells because of protein content and can also lead to dissolution and microstructural transformation of Zno [26-28]. Considering the above factors, aqueous medium devoid of any growth media was chosen to perform the antibacterial tests.

A graphical representation of the results of viability of *E. coli* strain after treatment with Zno Np dispersions (1mg mL^{-1}) is shown in Figure 3. The corresponding digital photograph is presented along with the plot in the inset. It can be observed that the sample at 0min shows a confluent growth. The colony count in this sample was therefore taken as 100% and the number of viable colonies in the other plates were compared to it at different time intervals. It is obvious that with increase in time, there is a dramatic decrease in the number of viable cell counts as shown in the inset. Although a considerable number of viable colonies can be observed in the plate at 60min with Zno Np, there is a significant reduction in viable cell counts compared to the sample at 0 min. It can be observed that the ZnO samples inactivate *E. coli* cells by more than 90% within 60min.

Figure 3: Kinetic plot of the antibacterial activity of the ZnO Np recorded at different time intervals.
Inset: Bacterial colonies of E. coli as after (a) 0min and (b) 60min treatment with ZnO Np.

The overall charge on bacteria and spore cell surfaces is negative at physiological pH due to the presence of an excess of carboxyl and other groups which upon dissociation render the cell surface negative [29]. Stoimenov et al. [29] have established from zeta potential measurements that the metal oxide suspensions are positively charged. The opposite charges on bacterial cell and Np cause electrostatic attraction between the two and the Np get tightly bound to the cell surface. The Np have an abrading effect on the bacterial cell surfaces and prolonged interaction causes disruption of cell wall and the underneath membrane resulting in leaching out of the protoplasmic contents. The abrasiveness of the Np is caused by an uneven surface structure due to rough edges and corners which can cause mechanical damage to the

bacterial cells [30]. In addition to above, the presence of defects on Zno Np surface also contributes to the antibacterial activity. A number of workers have established the presence of singly ionized oxygen vacancy (oxygen vacancy with one electron; $V_O^{\bullet}$) on Zno surface by EPR studies [31].

The atmospheric oxygen can combine with an electron on the Zno surface to produce a superoxide radical ($\cdot O_2^-$). The superoxide radical undergoes solvation in water to form a hydroperoxyl radical ($\cdot HO_2$) which can recombine to form H_2O_2. The H_2O_2 may further react with superoxide radical to produce hydroxyl radical ($\cdot OH$) and hydroxide ion (OH^-) [32]. The hydroxyl and superoxide radicals formed above are negatively charged particles and hence are unable to penetrate through the cell membrane whereas H_2O_2 can easily enter the cell. H_2O_2 can cause an oxidative stress which can damage DNA, cell membrane and proteins present inside causing cell death.

Conclusion

The present work proposes a methodology for a simple and scalable synthesis of Zno nanostructures using a microwave facilitated hydrothermal method. The method produces uniform size (~100nm) Zno Np. The synthesized Zno Np can successfully inhibit the growth of the Gram -ve bacterium *E. coli.* The bacteriostatic activity of Zno Np is expected to arise from mechanical interactions with cell surface and due to creation of oxidative stress by the reactive oxygen species produced from the surface defects of Zno Np. Thus, it is illustrated that the microwave synthesized Zno Np in the present work are promising candidates as antibacterial agents.

Acknowledgement

References

1. Cohen ML (1992) Epidemiology of drug resistance: Implications for a post-antimicrobial era. Science 257(5073): 1050-1055.

2. Xu X, Chen D, Yi Z, Jiang M, Wang L, et al. (2013) Antimicrobial mechanism based on H_2O_2 generation at oxygen vacancies in ZnO crystals. Langmuir 29(18): 5573-5580.

3. Manna AC (2012) Synthesis, characterization, and antimicrobial activity of zinc oxide nanoparticles. In: Cioffi N, Rai M (Eds.), Nano-Antimicrobials - Progress and Prospects, Springer, New York, USA, pp. 151-180.

4. Prasanna VL, Vijayaraghavan R (2015) Insight into the mechanism of antibacterial activity of Zno: Surface defects mediated reactive oxygen species even in the dark. Langmuir 31(33): 9155-9162.

5. Raghupathi KR, Koodali RT, Manna AC (2011) Size-dependent bacterial growth inhibition and mechanism of antibacterial activity of zinc oxide nanoparticles. Langmuir 27(7): 4020-4028.

6. Coleman VA, Jagadish C (2006) Basic properties and applications of Zno. In: Jagadish C, Pearton SJ (Eds.), Zinc Oxide Bulk, Thin Films and Nanostructures (1st edn), Elsevier, Netherlands, pp. 1-20.

7. Özgür Ü, Alivov Ya I, Liu C, Teke A, Reshchikov MA, et al. (2005) A comprehensive review of ZnO materials and devices. J Appl Phys 98: 041301.

8. Herring NP, Panda AB, Zeid KA, Almahoudi SH, Olson CR, et al. (2013) Microwave synthesis of metal oxide nanoparticles. In: Carpenter MA, Mathur S, Kolmakov A (Eds.), Metal Oxide Nanomaterials for Chemical Sensors. Springer Science+Business Media New York, USA, pp. 245-284.

9. Lidström P, Tierney J, Wathey B, Westman J (2001) Microwave assisted organic synthesis-a review. Tetrahedron 57(45): 9225-9283.

10. Kappe CO (2004) Controlled microwave heating in modern organic synthesis. Angew Chem Int Ed Engl 43(46): 6250-6284.

11. Polshettiwar V, Varma RS (2008) Aqueous microwave chemistry: a clean and green synthetic tool for rapid drug discovery. Chem Soc Rev 37(8): 1546-1557.

12. Liang M-K, Limo MJ, Sola RA, Roe MJ, Perry CC (2014) New insights into the mechanism of Zno formation from aqueous solutions of zinc acetate and zinc nitrate. Chem Mater 26(14): 4119-4129.

13. Demir MM, Munõz ER, Lieberwirth I, Wegner G (2006) Precipitation of monodisperse Zno nanocrystals via acid-catalyzed esterification of zinc acetate. J Mater Chem 16(28): 2940-2947.

14. Aimable A, Buscaglia MT, Buscaglia V, Bowen P (2010) Polymer-assisted precipitation of Zno nanoparticles with narrow particle size distribution. J Eur Ceram Soc 30(2): 591-598.

15. Moura AP, Lima RC, Moreira ML, Volanti DP, Espinosa JWM, et al. (2010) Zno architectures synthesized by a microwave-assisted hydrothermal method and their photoluminescence properties. Solid State Ionics 181(15): 775-780.

16. Krishnakumar T, Jayaprakash R, Pinnac N, Donato N, Bonavita A, et al. (2009) CO gas sensing of Zno nanostructures synthesized by an assisted microwave wet chemical route. Sens Actuators B 143(1): 198-204.

17. Liu J-S, Cao J-M, Li Z-Q, Ji G-B, Zheng M-B (2007) A simple microwave-assisted decomposing route for synthesis of Zno nanorods in the presence of PEG400. Mater Lett 61(22): 4409-4411.

18. Herring NP, Panchakarla LS, Shall MS (2014) P-type nitrogen-doped Zno nanostructures with controlled shape and doping level by facile microwave synthesis. Langmuir 30(8): 2230-2240.

19. Kajbafvala A, Ghorbani H, Paravar A, Samberg JP, Kajbafvala E, et al. (2012) Effects of morphology on photocatalytic performance of zinc oxide nanostructures synthesized by rapid microwave irradiation methods. Superlattices and Microstruct 51(4): 512-522.

20. Applerot G, Lipovsky A, Dror R, Perkas N, Nitzan Y, et al. (2009) Enhanced antibacterial activity of nanocrystalline ZnO due to increased ROS-mediated cell injury. Adv Funct Mater 19(6): 842-852.

21. Wu JM, Kao WT (2015) Heterojunction nanowires of AgxZn1-xo-Zno photocatalytic and antibacterial activities under visible-light and dark conditions. J Phys Chem C 119(3): 1433-1441.

22. He W, Jia H, Cai J, Han X, Zheng Z, et al. (2016) Production of reactive oxygen species and electrons from photoexcited Zno and ZnS nanoparticles: A comparative study for unraveling their distinct photocatalytic activities. J Phys Chem C 120(6): 3187-3195.

23. Kumar R, Anandan S, Hembram K, Rao TN (2014) Efficient Zno-based visible-light-driven photocatalyst for antibacterial applications. ACS Appl Mater Interfaces 6(15): 13138-13148.

24. Díez PAM, Díez VAL (2014) Zno-Reinforced poly(3-hydroxybutyrate-co-3-hydroxyvalerate) bionanocomposites with antimicrobial function

for food packaging. ACS Appl Mater Interfaces 6(12): 9822-9834.

25. Díez PAM, Díez VAL (2015) Wound healing bionanocomposites based on castor oil polymeric films reinforced with chitosan-modified Zno nanoparticles. Biomacromolecules 16(9): 2631-2644.

26. Liu S, Killen E, Lim M, Gunawan C, Amal R (2014) The effect of common bacterial growth media on zinc oxide thin films: identification of reaction products and implications for the toxicology of ZnO. RSC Adv 4(9): 4363-4370.

27. Hwang SH, Song J, Jung Y, Kweon OY, Song H, et al. (2011) Electrospun Zno/TiO$_2$ composite nanofibers as a bactericidal agent. Chem Commun 47(32): 9164-9166.

28. Jalal R, Goharshadia EK, Abareshia M, Moosavic M, Yousefid A, et al. (2010) Zno nanofluids: Green synthesis, characterization, and antibacterial activity. Mat Chem Phy 121(1-2): 198-201.

29. Stoimenov PK, Klinger RL, Marchin GL, Klabunde KJ (2002) Metal oxide nanoparticles as bactericidal agents. Langmuir 18(17): 6679-6686.

30. Padmavathy N, Vijayaraghavan R (2008) Enhanced bioactivity of Zno nanoparticles-an antimicrobial study. Sci Technol Adv Mater 9(3): 035004.

31. Ischenko V, Polarz S, Grote D, Stavarache V, Fink K, et al. (2005) Zinc oxide nanoparticles with defects. Adv Funct Mater 15(12): 1945-1954.

32. Blanksby SJ, Bierbaum VM, Ellison GB, Kato S (2007) Superoxide does react with peroxides: Direct observation of the Haber-Weiss reaction in the gas phase. Angew Chem Int Ed 46(26): 4948-4950.